



IUCrData

ISSN 2414-3146

Accurate intensity integration in the twinned γ -form of *o*-nitroaniline

Martin Lutz and Loes Kroon-Batenburg*

Department of Chemistry, Structural Biochemistry, Bijvoet Centre for Biomolecular Research, Faculty of Science, Utrecht University, Utrecht, The Netherlands. *Correspondence e-mail: l.m.j.kroon-batenburg@uu.nl

Received 5 July 2022

Accepted 3 November 2022

Edited by S. J. Coles, University of Southampton, United Kingdom

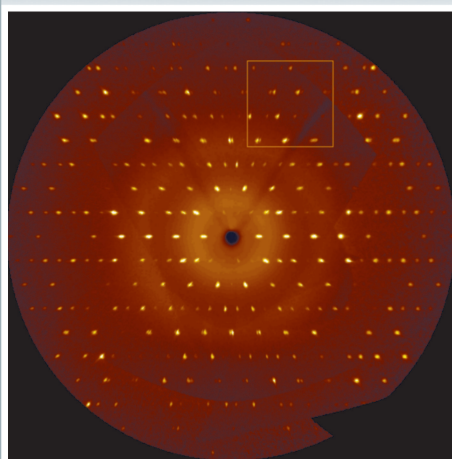
Keywords: twinning; scattering; twin interface; raw data.

CCDC reference: 2217206

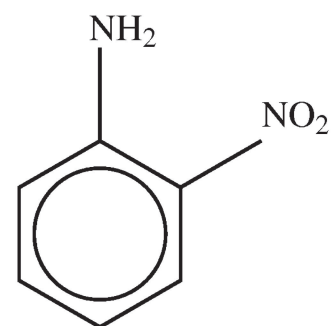
Structural data: full structural data are available from iucrdata.iucr.org

o-Nitroaniline, $C_6H_6N_2O_3$, is known to be polymorphic. The α -form is probably amorphous, while the β - and γ -forms are crystalline. Difficulties with the unit-cell determination of the γ -form were reported as a consequence of twinning. In this paper, newly recorded diffraction data of the γ -form of *o*-nitroaniline are described that were processed taking into account the two twin lattices. Data were partly deconvoluted and much better agreement was obtained in terms of R_1 values and C—C bond precision. The availability of raw data and proper reprocessing using twin lattices is by far superior to efforts to de-twin processed structure factors.

Raw data



Chemical



Bruker SMART data files and CBF files: <https://doi.org/10.5281/zenodo.7193538>

Metadata imgCIF file: <https://doi.org/10.1107/S2414314622010598/ii4001img.cif>

Introduction

o-Nitroaniline is known to be polymorphic (Aakeröy *et al.*, 1998*a,b*). The α -form is probably amorphous, while the β - and γ -forms are crystalline. Difficulties with the unit-cell determination of the γ -form were reported as a consequence of twinning. The unit cell appears to be *C*-centered orthorhombic, but was determined to be a pseudo-merohedral monoclinic twin by Herbstein (1965), who also observed diffuse streaks along a^* . Pseudo-orthorhombic twinning together with unusual extinctions was discussed by Dunitz (1964). While he assumed a twin obliquity of 0° , we here show an example where this is not exactly the case, *i.e.* the twin obliquity is 0.743° . The structure was determined before, supposedly from data of untwinned crystals, but the R_1 values of 10.9, 7.01 and 7.98% remain large (Dhaneshwar *et al.*, 1978; Nieger, 2007; Zych *et al.*, 2007). In this paper we describe newly recorded diffraction data of the γ -form of *o*-nitroaniline (I) and

Table 1
Experimental details.

Raw data			
DOI	https://doi.org/10.5281/zenodo.7193538		
Data archive	Zenodo		
Data format	CBF		
Data collection			
Diffractometer	Bruker Kappa APEXII		
Temperature (K)	150		
Detector type	APEXII CCD		
Radiation type	Mo $K\alpha$		
Wavelength (Å)	0.71073		
Beam center (mm)	−30.401, −30.637		
Detector axis	−Z		
Detector distance (mm)	41		
Swing angle (°)	−21.52		
Pixel size (µm)	0.12 × 0.12		
No. of pixels	512 × 512		
No. of scans	7		
Exposure time per frame (s)	10		
Scan axis	Start angle, increment per frame (°)	Scan range (°)	No. of frames
ϕ , $-X$ ($\omega = 164.659^\circ$, $\kappa = 46.226^\circ$)	74.659, −0.300	−360	1200
ω , $-X$ ($\kappa = -73.760^\circ$, $\phi = 10.746^\circ$)	−169.393, −0.300	−118.2	394
ω , $-X$ ($\kappa = -73.760^\circ$, $\phi = -91.253^\circ$)	−169.393, −0.300	−118.2	394
ω , $-X$ ($\kappa = 88.307^\circ$, $\phi = 160.033^\circ$)	−157.189, −0.300	−82.2	274
ω , $-X$ ($\kappa = 88.307^\circ$, $\phi = 58.033^\circ$)	−157.189, −0.300	−82.2	274
ω , $-X$ ($\kappa = -73.760^\circ$, $\phi = -40.253^\circ$)	−169.393, −0.300	−118.2	394
ω , $-X$ ($\kappa = -73.760^\circ$, $\phi = 166.747^\circ$)	−169.393, −0.300	−118.2	394
Crystal data			
Chemical formula	$C_6H_6N_2O_2$		
M_r	138.13		
Crystal system, space group	Monoclinic, $P21/a$		
a , b , c (Å)	15.2066 (5), 10.0938 (4), 8.3580 (2)		
β (°)	106.693 (3)		
V (Å ³)	1228.82 (7)		
Z	8		
μ (mm ^{−1})	0.12		
Crystal size (mm)	0.37 × 0.30 × 0.16		
Data processing			
Absorption correction	Twin Multi-scan (<i>TWINABS2012/I</i> ; Sevvana <i>et al.</i> , 2019)	Single lattice Multi-scan (<i>SADABS</i> ; Krause <i>et al.</i> , 2015)	
T_{\min} , T_{\max}	0.683, 0.746	0.628, 0.746	
No. of measured, independent and observed [$I > 2\sigma(I)$] reflections	26077, 2864, 2629 2145 overlapping and 842 single reflections and 123 systematic absences	24760, 2816, 2547	
R_{int}	0.028	0.034	
$(\sin \theta/\lambda)_{\text{max}}$ (Å ^{−1})	0.655	0.655	
Refinement			
No. of reflections	2864	2816	
No. of parameters	198	197	
H-atom treatment	N—H refined freely; C—H refined with a riding model	N—H refined freely; C—H refined with a riding model	
$R[F^2 > 2\sigma(F^2)]$, $wR(F^2)$, S	0.0314, 0.0860, 1.085	0.0787, 0.2545, 1.154	
Twin fraction BASF	0.2003 (10)		
Weighting scheme	$a = 0.0449$, $b = 0.2210$	$a = 0.0702$, $b = 6.2812$	
$\Delta\rho_{\text{max}}$, $\Delta\rho_{\text{min}}$ (e Å ^{−3})	0.23, −0.22	0.35, −0.36	
Bond precision C—C (Å)	0.0017	0.0062	

process these by taking into account the two twin lattices. We show that the availability of raw data and proper reprocessing using twin lattices is by far superior to efforts to de-twin processed structure factors.

Data processing and refinement

Data were processed in two ways: by using a single lattice, ignoring the second lattice completely, and by using two twin

lattices. *EVAL* software (Schreurs *et al.*, 2010) was used for both, followed by *SADABS/TWINABS* (Krause *et al.*, 2015; Sevvana *et al.*, 2019) for scaling. Splitting of the radiation in $K\alpha_1$ and $K\alpha_2$ in a 2:1 ratio is taken into account in the *EVAL* model profiles for either lattice. The statistics for the two approaches are given in Table 1. Several indicators in the single-crystal data processing show that the crystal is not a single crystal. The first real sign of an alarm occurs when it comes to the space-group determination: the most likely space

group is $P2_1/a$ but systematic absences for the a -glide plane are clearly violated (reflection condition $h0l$; $h = 2n$). Structure refinement with *SHELXL* (Sheldrick, 2015) converges at high residuals $R_1[I > 2\sigma(I)] = 0.0787$ and $wR_2(\text{all refl.}) = 0.2545$ and the proposed weighting scheme is rather unusual. The two twin lattices are related by a twofold rotation about c , resulting in the twin matrix $\begin{pmatrix} -1 & 0 & -1 \\ 0 & -1 & 0 \\ 0 & 0 & 1 \end{pmatrix}$ (see below). With only single-crystal structure factors it is still possible to use the knowledge of the twin matrix. Inclusion of this matrix in the *SHELXL* refinement assumes that the lattices overlap exactly and the obliquity would be 0° . In reality, not all reflections overlap and thus the refinement results improve only slightly [$R_1[I > 2\sigma(I)] = 0.0678$ and $wR_2(\text{all refl.}) = 0.2390$]. As a last resort, one can de-twin the merged data with *TWINROT* in *PLATON* (Spek, 2020). This produces an HKLF5-type file for refinement in *SHELXL* in which each reflection is either overlapped or single (935 reflections are overlapping). The structure refinement improved to $R_1[I > 2\sigma(I)] = 0.0465$ and $wR_2(\text{all refl.}) = 0.1332$. As we will see below, it is a poor approach for resolving the twinning issue with *processed* data, clearly *raw* diffraction data are needed to reprocess with two lattices.

To show the advantage of proper processing we used two matrices. One twin component was clearly the largest and we processed the data with this lattice while including the second lattice as interfering in *EVAl*. Reflections are deconvoluted when the covariance of the overlapping intensities is below a given threshold. This led to 2145 overlapping and 842 single reflections and 123 systematic absences (Table 1). The agreement factors of the *SHELXL* refinement are much improved to $R_1[I > 2\sigma(I)] = 0.0314$ and $wR_2(\text{all refl.}) = 0.0860$ (Table 1) and the displacement ellipsoids of the two independent molecules are perfectly reasonable (Fig. 1).

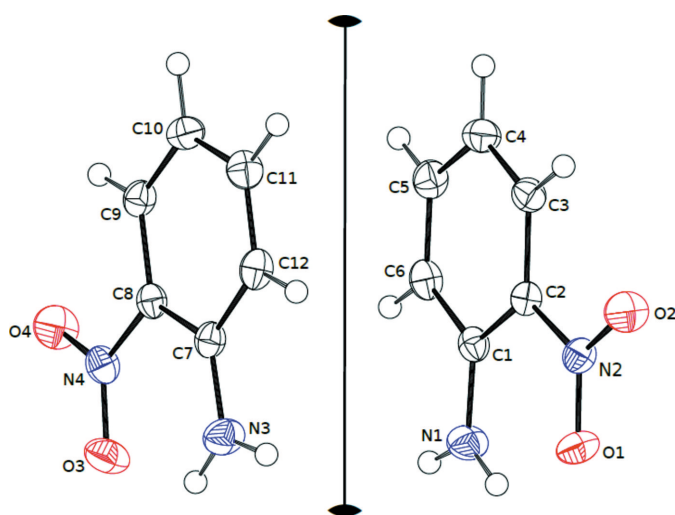


Figure 1
Molecular structure of the two independent molecules of (I) in the crystal. Displacement ellipsoids are drawn at the 50% probability level. Hydrogen atoms are drawn as small spheres of arbitrary radii. The molecules are related by a non-crystallographic twofold axis approximately along a^* .

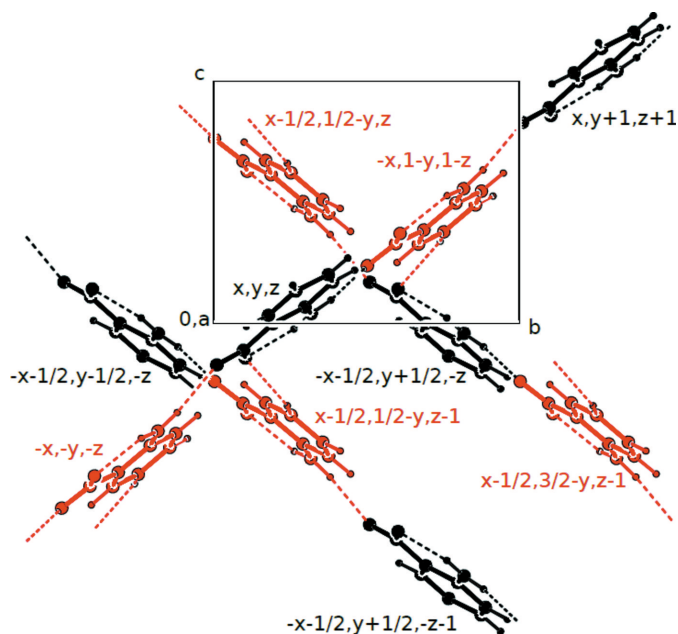


Figure 2
Hydrogen-bonded layers in the monoclinic structure.

The crystal structure has $P2_1/a$ symmetry with two independent molecules, which are shown in Fig. 1. The molecules are connected by hydrogen bonds, forming two-dimensional layers in the bc plane (Fig. 2).

Data description

Data were collected on our in-house *APEXII* diffractometer with Mo $K\alpha$ radiation, with multiple scans (Table 1). In total 3324 images were recorded. The unit cell was determined with *DIRAX* (Duisenberg, 1992) and two lattices were found that could be transformed into each other with a nearly twofold rotation. Pseudo-orthorhombic twinning is characterized by a base-centered orthorhombic twin lattice derived from a monoclinic- P crystal lattice (Dunitz, 1964). The monoclinic P cell of (I) can be transformed to a near orthorhombic B lattice [the non-standard setting of the space group $P2_1/a$ was chosen for compatibility with earlier literature (Herbstein, 1965); base-centered B -orthorhombic was chosen so as to leave b and c unchanged] with the following operation:

$$\begin{pmatrix} \mathbf{a}' \\ \mathbf{b}' \\ \mathbf{c}' \end{pmatrix} = \begin{pmatrix} 2 & 0 & 1 \\ 0 & 1 & 0 \\ 0 & 0 & 1 \end{pmatrix} \begin{pmatrix} \mathbf{a} \\ \mathbf{b} \\ \mathbf{c} \end{pmatrix}$$

giving cell parameters $a' = 29.1340(10)$, $b' = 10.0938(4)$, $c' = 8.3580(2)$, Å, $\alpha' = 90^\circ$, $\beta' = 90.743(3)$, $\gamma' = 90^\circ$. The c axis was chosen as the twofold twin rotation axis. Clearly we find a twin obliquity of $0.743(3)^\circ$ and a non-merohedral twin. As a consequence, the orthorhombic B lattices of the individual twin components do not exactly overlap. If one overlooks the twinning and indexes the spots as B -centered orthorhombic in space group $B22_12$, the reflection conditions appear to be: hkl ; $h + l = 2n$, $0k0$; $k = 2n$, which is usual for the space group,

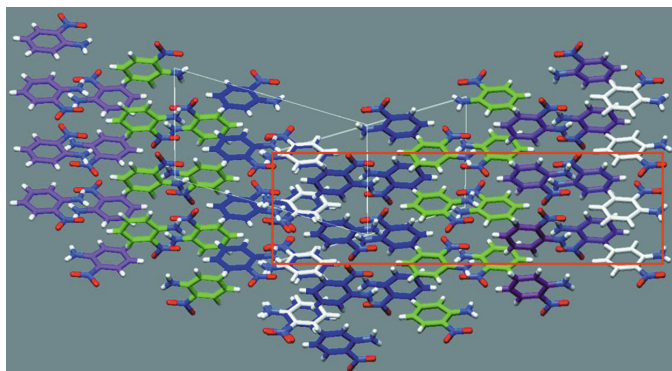


Figure 3

Twin domains viewed down the monoclinic b -axis, with alternate layers colored in white, blue, green and magenta. The layers have a width of two hydrogen-bonded molecules (see Fig. 2) and have hydrophobic faces. The second lattice (left) has a row of molecules in the blue layer in common with that of the white layer in the first lattice (right). The second domain is generated by a twofold rotation around c and a shift over $1/2a$. The pseudo-orthorhombic unit cell is shown in red. The hydrophobic interactions between the layers are almost completely conserved across the twin interface.

and $h00$; $h = 4n$, $00l$; $l = 4n$. The latter two are non-space-group extinctions and exactly such observations are considered as a signal for pseudo-orthorhombic twinning of an underlying monoclinic lattice (Dunitz, 1964). Processing the data as single-component orthorhombic does not result in a structure solution, notably because the a glide plane is absent in $B22_12$.

The twin rotation about the c -axis results in stacking faults of the hydrogen-bonded layers. In Fig. 3, the two domains and the twinning interface is shown. The second lattice was generated by 180° rotation around c followed by a translation over $1/2a$, by which the two independent molecules are interchanged in the position. In fact, the two molecules can almost be transformed into each other by a twofold rotation along a' , the long orthorhombic axis, showing that this axis is a near orthorhombic twofold axis. The twinning and stacking faults follow the OD theory as proposed by Dornberger-Schiff (1966) for similar systems.

As a consequence of the twin obliquity $\omega = 0.743 (3)^\circ$, reflections are split in reciprocal space. This can be seen in simulated precession photographs that were generated with

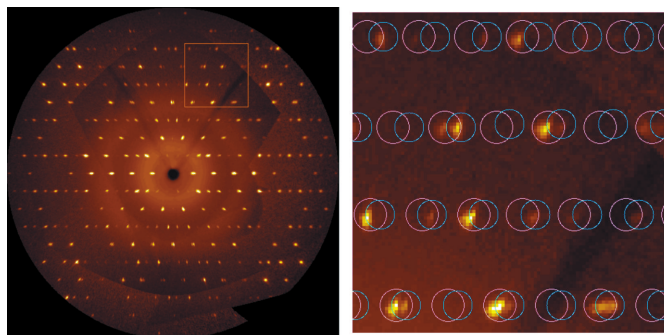


Figure 4

Left: simulated precession photograph in the $h0l$ plane of (I) up to a resolution of 0.9 \AA . The reconstruction is based on seven scans with a total of 3324 raw images. Right: zoomed image, is from the yellow square in the left image. White circles are the predicted impacts for the first twin component, blue circles for the second.

the program *PRECESSION* in the *EVAL* package. In the $0th$ layers, this mainly affects layer $h0l$ (Fig. 4). In the layers, $hk0$ and $0kl$ reflections remain nearly unaffected.

References

- Aakeröy, C. B., Nieuwenhuyzen, M. & Price, S. L. (1998a). *J. Am. Chem. Soc.* **120**, 8986–8993.
- Aakeröy, C. B., Beatty, A. M., Nieuwenhuyzen, M. & Zou, M. (1998b). *J. Mater. Chem.* **8**, 1385–1389.
- Dhaneshwar, N. N., Tavale, S. S. & Pant, L. M. (1978). *Acta Cryst.* **B34**, 2507–2509.
- Dornberger-Schiff, K. (1966). *Acta Cryst.* **21**, 311–322.
- Duisenberg, A. J. M. (1992). *J. Appl. Cryst.* **25**, 92–96.
- Dunitz, J. D. (1964). *Acta Cryst.* **17**, 1299–1304.
- Herbstein, F. H. (1965). *Acta Cryst.* **19**, 590–595.
- Krause, L., Herbst-Irmer, R., Sheldrick, G. M. & Stalke, D. (2015). *J. Appl. Cryst.* **48**, 3–10.
- Nieger, M. (2007). *CSD Communication* (CCDC No. 655336). CCDC, Cambridge, England.
- Schreurs, A. M. M., Xian, X. & Kroon-Batenburg, L. M. J. (2010). *J. Appl. Cryst.* **43**, 70–82.
- Sevvana, M., Ruf, M., Usón, I., Sheldrick, G. M. & Herbst-Irmer, R. (2019). *Acta Cryst.* **D75**, 1040–1050.
- Sheldrick, G. M. (2015). *Acta Cryst.* **C71**, 3–8.
- Spek, A. L. (2020). *Acta Cryst.* **E76**, 1–11.
- Zych, T., Misiaszek, T. & Szostak, M. M. (2007). *Chem. Phys.* **340**, 260–272.

full crystallographic data

IUCrData (2022). 7, x221059 [https://doi.org/10.1107/S2414314622010598]

Accurate intensity integration in the twinned γ -form of *o*-nitroaniline

Martin Lutz and Loes Kroon-Batenburg

(I)

Crystal data

$C_6H_6N_2O_2$	$F(000) = 576$
$M_r = 138.13$	$D_x = 1.493 \text{ Mg m}^{-3}$
Monoclinic, $P2_1/a$	Mo $K\alpha$ radiation, $\lambda = 0.71073 \text{ \AA}$
$a = 15.2066 (5) \text{ \AA}$	Cell parameters from 9064 reflections
$b = 10.0938 (4) \text{ \AA}$	$\theta = 2.5\text{--}27.5^\circ$
$c = 8.3580 (2) \text{ \AA}$	$\mu = 0.12 \text{ mm}^{-1}$
$\beta = 106.693 (3)^\circ$	$T = 150 \text{ K}$
$V = 1228.82 (7) \text{ \AA}^3$	Block, orange
$Z = 8$	$0.37 \times 0.30 \times 0.16 \text{ mm}$

Data collection

Bruker Kappa APEXII Area Detector diffractometer	2864 independent reflections
Radiation source: sealed tube	2629 reflections with $I > 2\sigma(I)$
φ and ω scans	$R_{\text{int}} = 0.028$
Absorption correction: multi-scan (TWINABS2012/1; Sevvana, 2019)	$\theta_{\text{max}} = 27.8^\circ$, $\theta_{\text{min}} = 2.5^\circ$
$T_{\text{min}} = 0.683$, $T_{\text{max}} = 0.746$	$h = -19 \rightarrow 19$
26077 measured reflections	$k = -13 \rightarrow 13$
	$l = -10 \rightarrow 10$

Refinement

Refinement on F^2	Secondary atom site location: difference Fourier map
Least-squares matrix: full	Hydrogen site location: difference Fourier map
$R[F^2 > 2\sigma(F^2)] = 0.031$	H atoms treated by a mixture of independent and constrained refinement
$wR(F^2) = 0.086$	$w = 1/[\sigma^2(F_o^2) + (0.0449P)^2 + 0.221P]$
$S = 1.09$	where $P = (F_o^2 + 2F_c^2)/3$
2864 reflections	$(\Delta/\sigma)_{\text{max}} < 0.001$
198 parameters	$\Delta\rho_{\text{max}} = 0.23 \text{ e \AA}^{-3}$
0 restraints	$\Delta\rho_{\text{min}} = -0.22 \text{ e \AA}^{-3}$
Primary atom site location: structure-invariant direct methods	

Special details

Geometry. All esds (except the esd in the dihedral angle between two l.s. planes) are estimated using the full covariance matrix. The cell esds are taken into account individually in the estimation of esds in distances, angles and torsion angles; correlations between esds in cell parameters are only used when they are defined by crystal symmetry. An approximate (isotropic) treatment of cell esds is used for estimating esds involving l.s. planes.

Refinement. Refined as a 2-component twin.

Fractional atomic coordinates and isotropic or equivalent isotropic displacement parameters (\AA^2)

	<i>x</i>	<i>y</i>	<i>z</i>	$U_{\text{iso}}^*/U_{\text{eq}}$
O1	−0.03312 (6)	0.10319 (9)	−0.14230 (11)	0.0285 (2)
O2	0.08962 (6)	0.01027 (9)	−0.17072 (12)	0.0324 (2)
N1	−0.02204 (7)	0.31912 (12)	0.04086 (15)	0.0285 (2)
H1	−0.0624 (13)	0.2625 (19)	−0.023 (2)	0.049 (5)*
H2	−0.0380 (10)	0.3830 (16)	0.096 (2)	0.027 (4)*
N2	0.05199 (7)	0.09765 (10)	−0.11006 (12)	0.0218 (2)
C1	0.06867 (8)	0.29873 (11)	0.06793 (13)	0.0204 (2)
C2	0.10796 (7)	0.19361 (11)	−0.00104 (13)	0.0193 (2)
C3	0.20382 (8)	0.17923 (12)	0.03417 (14)	0.0228 (2)
H3	0.228408	0.106997	−0.011917	0.027*
C4	0.26139 (8)	0.26863 (13)	0.13415 (15)	0.0267 (3)
H4	0.326021	0.259080	0.158007	0.032*
C5	0.22411 (8)	0.37519 (12)	0.20167 (15)	0.0257 (2)
H5	0.264081	0.438511	0.269680	0.031*
C6	0.13135 (8)	0.38906 (12)	0.17098 (14)	0.0237 (2)
H6	0.108260	0.461106	0.219982	0.028*
O3	−0.01284 (6)	0.39005 (10)	0.62855 (13)	0.0325 (2)
O4	0.10944 (7)	0.49706 (9)	0.76124 (12)	0.0344 (2)
N3	−0.00207 (8)	0.18216 (12)	0.44357 (14)	0.0294 (2)
H7	−0.0423 (12)	0.2364 (18)	0.473 (2)	0.045 (5)*
H8	−0.0209 (10)	0.1190 (16)	0.367 (2)	0.026 (4)*
N4	0.07189 (7)	0.40432 (10)	0.67046 (12)	0.0234 (2)
C7	0.08863 (8)	0.20773 (12)	0.50315 (14)	0.0209 (2)
C8	0.12800 (7)	0.31208 (11)	0.61380 (13)	0.0196 (2)
C9	0.22377 (8)	0.32999 (12)	0.67275 (14)	0.0222 (2)
H9	0.248337	0.400078	0.748209	0.027*
C10	0.28159 (8)	0.24690 (12)	0.62182 (15)	0.0251 (2)
H10	0.346191	0.258978	0.661043	0.030*
C11	0.24405 (8)	0.14352 (12)	0.51074 (15)	0.0253 (2)
H11	0.283938	0.086081	0.474351	0.030*
C12	0.15120 (8)	0.12380 (12)	0.45380 (14)	0.0240 (2)
H12	0.128075	0.052375	0.379621	0.029*

Atomic displacement parameters (\AA^2)

	U^{11}	U^{22}	U^{33}	U^{12}	U^{13}	U^{23}
O1	0.0200 (4)	0.0292 (4)	0.0320 (4)	−0.0006 (3)	0.0006 (4)	−0.0038 (4)
O2	0.0317 (4)	0.0275 (4)	0.0373 (5)	0.0010 (4)	0.0088 (4)	−0.0141 (4)
N1	0.0233 (5)	0.0293 (5)	0.0332 (5)	0.0051 (4)	0.0086 (4)	−0.0072 (5)
N2	0.0237 (4)	0.0198 (4)	0.0208 (4)	0.0002 (4)	0.0047 (4)	−0.0010 (4)
C1	0.0240 (5)	0.0189 (5)	0.0193 (5)	0.0028 (4)	0.0078 (4)	0.0029 (4)
C2	0.0220 (5)	0.0173 (5)	0.0183 (5)	−0.0003 (4)	0.0054 (4)	−0.0001 (4)
C3	0.0231 (5)	0.0233 (5)	0.0231 (5)	0.0029 (4)	0.0081 (4)	−0.0015 (4)
C4	0.0213 (5)	0.0304 (6)	0.0285 (6)	−0.0015 (5)	0.0075 (5)	−0.0029 (5)
C5	0.0289 (6)	0.0242 (6)	0.0239 (5)	−0.0061 (5)	0.0077 (5)	−0.0037 (5)

C6	0.0317 (6)	0.0183 (5)	0.0228 (5)	0.0011 (4)	0.0108 (5)	-0.0018 (4)
O3	0.0245 (4)	0.0345 (5)	0.0420 (5)	-0.0003 (4)	0.0151 (4)	-0.0080 (4)
O4	0.0367 (5)	0.0275 (5)	0.0402 (5)	-0.0031 (4)	0.0129 (4)	-0.0154 (4)
N3	0.0248 (5)	0.0297 (5)	0.0318 (5)	-0.0026 (4)	0.0049 (4)	-0.0098 (5)
N4	0.0281 (5)	0.0204 (5)	0.0238 (5)	-0.0003 (4)	0.0107 (4)	-0.0018 (4)
C7	0.0251 (5)	0.0192 (5)	0.0182 (5)	-0.0009 (4)	0.0057 (4)	0.0018 (4)
C8	0.0237 (5)	0.0175 (5)	0.0184 (5)	0.0009 (4)	0.0075 (4)	0.0009 (4)
C9	0.0253 (5)	0.0203 (5)	0.0200 (5)	-0.0035 (4)	0.0050 (4)	-0.0011 (4)
C10	0.0204 (5)	0.0268 (6)	0.0267 (5)	0.0001 (4)	0.0043 (4)	0.0014 (5)
C11	0.0289 (6)	0.0217 (5)	0.0263 (5)	0.0056 (4)	0.0093 (5)	0.0012 (5)
C12	0.0319 (6)	0.0182 (5)	0.0211 (5)	-0.0002 (4)	0.0065 (5)	-0.0026 (4)

Geometric parameters (Å, °)

O1—N2	1.2451 (12)	O3—N4	1.2428 (12)
O2—N2	1.2366 (13)	O4—N4	1.2365 (13)
N1—C1	1.3479 (14)	N3—C7	1.3499 (15)
N1—H1	0.89 (2)	N3—H7	0.906 (18)
N1—H2	0.867 (17)	N3—H8	0.892 (16)
N2—C2	1.4308 (14)	N4—C8	1.4323 (14)
C1—C6	1.4178 (16)	C7—C8	1.4159 (16)
C1—C2	1.4188 (15)	C7—C12	1.4209 (16)
C2—C3	1.4093 (14)	C8—C9	1.4086 (15)
C3—C4	1.3633 (17)	C9—C10	1.3684 (16)
C3—H3	0.9500	C9—H9	0.9500
C4—C5	1.4073 (17)	C10—C11	1.4043 (17)
C4—H4	0.9500	C10—H10	0.9500
C5—C6	1.3664 (16)	C11—C12	1.3689 (16)
C5—H5	0.9500	C11—H11	0.9500
C6—H6	0.9500	C12—H12	0.9500
C1—N1—H1	119.9 (12)	C7—N3—H7	118.8 (11)
C1—N1—H2	117.0 (10)	C7—N3—H8	119.0 (9)
H1—N1—H2	122.8 (15)	H7—N3—H8	121.8 (15)
O2—N2—O1	121.19 (10)	O4—N4—O3	121.29 (10)
O2—N2—C2	118.90 (9)	O4—N4—C8	118.75 (9)
O1—N2—C2	119.91 (9)	O3—N4—C8	119.95 (9)
N1—C1—C6	118.74 (10)	N3—C7—C8	125.36 (11)
N1—C1—C2	125.17 (11)	N3—C7—C12	118.51 (11)
C6—C1—C2	116.08 (10)	C8—C7—C12	116.12 (10)
C3—C2—C1	121.55 (10)	C9—C8—C7	121.65 (10)
C3—C2—N2	116.98 (9)	C9—C8—N4	117.07 (10)
C1—C2—N2	121.47 (9)	C7—C8—N4	121.28 (10)
C4—C3—C2	120.22 (11)	C10—C9—C8	120.30 (10)
C4—C3—H3	119.9	C10—C9—H9	119.8
C2—C3—H3	119.9	C8—C9—H9	119.8
C3—C4—C5	119.34 (11)	C9—C10—C11	119.06 (11)
C3—C4—H4	120.3	C9—C10—H10	120.5

C5—C4—H4	120.3	C11—C10—H10	120.5
C6—C5—C4	121.06 (11)	C12—C11—C10	121.38 (10)
C6—C5—H5	119.5	C12—C11—H11	119.3
C4—C5—H5	119.5	C10—C11—H11	119.3
C5—C6—C1	121.72 (10)	C11—C12—C7	121.48 (11)
C5—C6—H6	119.1	C11—C12—H12	119.3
C1—C6—H6	119.1	C7—C12—H12	119.3
N1—C1—C2—C3	-179.80 (11)	N3—C7—C8—C9	178.63 (11)
C6—C1—C2—C3	1.17 (15)	C12—C7—C8—C9	-0.80 (16)
N1—C1—C2—N2	0.44 (17)	N3—C7—C8—N4	-1.47 (17)
C6—C1—C2—N2	-178.59 (10)	C12—C7—C8—N4	179.09 (10)
O2—N2—C2—C3	-1.88 (15)	O4—N4—C8—C9	3.00 (15)
O1—N2—C2—C3	178.13 (10)	O3—N4—C8—C9	-176.83 (10)
O2—N2—C2—C1	177.89 (10)	O4—N4—C8—C7	-176.90 (10)
O1—N2—C2—C1	-2.10 (16)	O3—N4—C8—C7	3.28 (16)
C1—C2—C3—C4	-1.19 (17)	C7—C8—C9—C10	0.93 (17)
N2—C2—C3—C4	178.58 (11)	N4—C8—C9—C10	-178.97 (10)
C2—C3—C4—C5	0.00 (18)	C8—C9—C10—C11	-0.25 (17)
C3—C4—C5—C6	1.16 (18)	C9—C10—C11—C12	-0.53 (18)
C4—C5—C6—C1	-1.16 (18)	C10—C11—C12—C7	0.64 (18)
N1—C1—C6—C5	-179.10 (11)	N3—C7—C12—C11	-179.45 (11)
C2—C1—C6—C5	-0.01 (16)	C8—C7—C12—C11	0.03 (16)

Hydrogen-bond geometry (Å, °)

<i>D</i> —H... <i>A</i>	<i>D</i> —H	H... <i>A</i>	<i>D</i> ... <i>A</i>	<i>D</i> —H... <i>A</i>
N1—H1...O1	0.89 (2)	2.010 (19)	2.6409 (15)	126.4 (16)
N1—H2...O4 ⁱ	0.867 (17)	2.194 (17)	3.0345 (14)	163.2 (14)
N3—H7...O3	0.906 (18)	1.989 (19)	2.6393 (15)	127.3 (15)
N3—H8...O2 ⁱⁱ	0.892 (16)	2.120 (16)	3.0003 (14)	169.0 (13)

Symmetry codes: (i) $-x, -y+1, -z+1$; (ii) $-x, -y, -z$.